JPE 9-3-15

ICPE'07 Selected Paper

The New Smart Power Modules for up to 1kW Motor Drive Application

Tae-Sung Kwon† and Sung-Il Yong*

†* Motion Control System Team, HV PCIA, Fairchild Semiconductor, Korea

ABSTRACT

This paper introduces a new Motion-SPM™ (Smart Power Modules) module in Single In-line Package (SIP), which is a fully optimized intelligent integrated IGBT inverter module for up to 1kW low power motor drive applications. This module offers a sophisticated, integrated solution and tremendous design flexibility. It also takes advantage of pliability for the arrangement of heat-sink due to two types of lead forms. It comes to be realized by employing non-punch-through (NPT) IGBT with a fast recovery diode and highly integrated building block, which features built-in HVICs and a gate driver that offers more simplicity and compactness leading to reduced costs and high reliability of the entire system. This module also provides technical advantages such as the optimized cost effective thermal performances through IMS (Insulated Metal Substrate), the high latch immunity. This paper provides an overall description of the Motion-SPM™ in SIP as well as actual application issues such as electrical characteristics, thermal performance, circuit configurations and power ratings.

Keywords: Motion-SPM™, Single In-line Package, NPT IGBT, Fast recovery diode, HVICs, Insulated Metal Substrate

1. Introduction

Motors are the major source of energy consumption in appliances. Since governmental and agency regulations continue to mandate reduced energy consumption, inverter technology is being increasingly accepted and used by a wide range of users in the design of their products. Power modules which integrate the discrete power semiconductors and drives into one package for inverterized motor drive applications are part of a current trend due to the offered advantages of reducing the development time, space-savings and ease of assembly. Also, these enable developers to accelerate their products time-to-market, bringing innovation to their end customers faster [1]-[2].

The Motion-SPM™ in SIP, which has been developed at this time, is quite specialized for an IGBT inverter application range of less than 1kW. Within such an operating power, one of the most important requirements in the system is more compactness and easier mass production process with high quality and reliability resulting in more cost-effectiveness compared to discrete inverter solutions. These modules have been fully developed as an answer to the strong demands, particularly in home appliances applications such as air-conditioners, and washing machines and refrigerators,

Manuscript received Jan. 31, 2009; revised April 3, 2009
†Corresponding Author: TaeSung.Kwon@fairchildsemi.co.kr
Tel:+81-32-680-1388, Fax:+82-32-680-1823, Fairchild
*Motion Control System Team, HV PCIA, Fairchild Semicond uctor, Korea

requiring higher efficiency and higher performance characteristics. This paper describes in detail the design issues, electrical performance, and other important considerations for designing the system.

2. Main Features of Design and Function

2.1 External view and Circuit Structure

Fig. 1 and 2 show a real photograph and internal equivalent circuit of the Motion-SPM^{TM} in SIP. The SIP package is composed of six NPT IGBTs, six freewheeling diodes, three HVICs, one LVIC and one thermistor. The NPT IGBTs are designed with key electrical characteristics such as low conduction/switching losses over all driving conditions, short circuit withstanding capability for the motor drive, and smooth switching waveforms without EMI noises caused by rapid dV/dt. The most important characteristics of the freewheeling diodes are soft recovery behavior over the whole current, temperature range and low forward voltage drop. System reliability is further enhanced due to internal temperature detection using a built-in thermistor, integrated under-voltage and short circuit lockout protection. The high-speed built-in HVIC enables the use of a single power supply without a photo coupler. One feature of the HVIC is its built-in high voltage level-shifting function that enables the PWM input from a microcontroller to be directly transferred to a high side power device. This results in size and cost reduction of the inverter systems.

The Motion-SPM^{TM} in SIP has two types of negative DC terminals. One has three divided negative DC terminals to monitor the inverter output current by using three external shunt resistors and to provide a sensor-less control solution. The other has one negative DC terminal to sense the DC-link current and short-circuit protection by using one external shunt resistor.

2.2 Functional Description

The Motion-SPM^{TM} module in SIP provides two main protective functions. One is to control supply under-voltage protection and the other is to control short-circuit current protection. When the control supply voltage drops under its UV detect level, the internal gating signal is blocked and a fault-out signal is generated. Once the supply voltage rises again over the UV reset level, the fault-out signal becomes high and the SPM® is operated by command signals. The Motion-SPM^{TM} module in SIP packaging can monitor the inverter leg current by using an external shunt resistor. The LVIC of the SPM® in SIP monitors the low-side collector current with the C_{SC} pin. If the voltage of the C_{SC} pin exceeds 0.5V, the internal gating signal is blocked and a fault-out signal is generated. Hence, the external shunt resistor can be selected to determine the trip current level, which can be optimized depending on the field requirements.

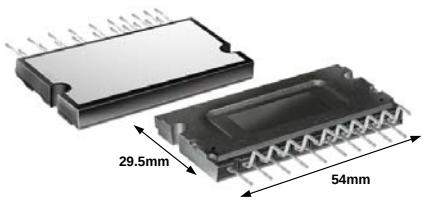

Fig. 1. Photograph of Motion-SPM^{TM} in SIP.

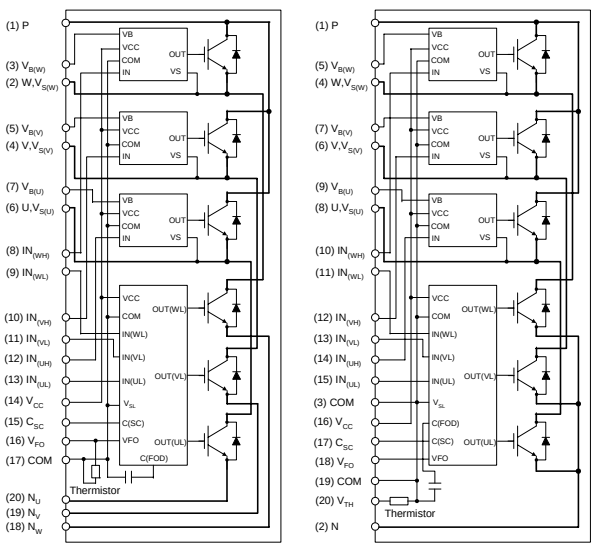

(a) (b)

Fig. 2. Internal equivalent circuit of Motion-SPM^{TM} in SIP. (a) 3-N Type (b) 1-N Type

Additionally, the Motion-SPM^{TM} module in SIP has a strong noise immunity characteristic due to the use of the HVICs adopted new technology. Fig. 3 shows the internal HVICs block of the Motion-SPM^{TM} module in SIP.

HVICs are generally sensitive to external noise since its signal is transferred by pulse signal and S-R latch [3]. A high dv/dt switching of a driven IGBT is especially the most dangerous type for this kind of pulse driven HVIC. Assuming the parasitic capacitance of the LDMOS seen at the drain is C_M and the on-dv/dt of a high side IGBT is dVS/dt, the C_M must be charged with the large current, C_M*dVS/dt, for the LDMOS drain voltage to follow the fast changing VB voltage, which is coupled to the VS by a bootstrap capacitor C_{BS}. The large charging current makes an excessive voltage drop on R1 and R2 to abnormally trigger the S-R latch. To overcome noise sensitivity, a noise canceller with a unique topology has been developed as shown in Fig. 3 [4]. The V/I converter converts the level shifter's outputs to the current information. For the common-mode noise, which has high dv/dt, the V/I converter gives the same outputs. Whereas, the V/I converter outputs are different from each other for normal operation, as only one of two LDMOSs operates at a normal level shifter operation. Thus, it is not difficult to determine whether the V/I converter output is due to noise or not. Once the noise canceller recognizes a common-mode noise intrusion, it absorbs the current outputs of the V/I converter. Then, the I/V converter reconstructs the voltage signal, which swings between VB and VS supply rails from the current outputs of the V/I converter. Finally, the amplified signal is sent to the S-R latch. Another merit of V/I and I/V conversion is that the allowable negative VS voltage is no longer governed by the threshold level of the circuit. Owing to its unique topology, the Fairchild HVIC demonstrates good noise immunity against high dv/dt noise of up to 50V/nsec and allows an extended negative operation of up to VS=-10V @ VBS=15V approximately.

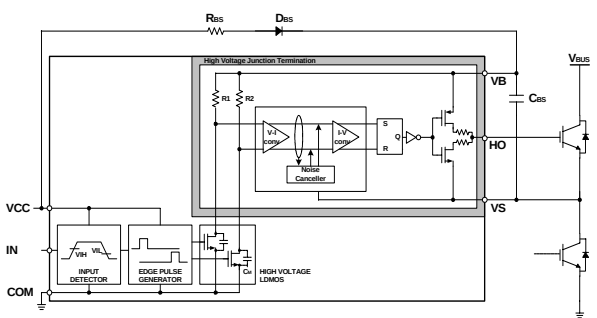

Fig. 3. High-side driver configuration.

2.3 Package Structure

The narrow space multi-die attach technology is used in the Motion-SPM™ in SIP. This results in reduced noise, size and less mutual interference. This package is designed to guarantee the best heat transfer from the power chips to the outer heat-sink by using an IMS package. The IMS substrate uses an aluminum plate at the base. The upper side of the substrate consists of a thermally conductive dielectric layer and a copper cladding on which the circuit is etched. This takes advantage of the high thermal conductivity and simple manufacturing. Fig. 4 shows the thermal impedances characteristics about the 600V/8A rating device of Motion-SPM™ in SIP.

The lead frame structure has a 1.385mm down-set shape. This structure makes the thermal resistance low but does not reduce the distance between lead frame and the outer heat-sink. More down-set thickness affects the reliability and assembly process. The optimization of the bending depth has been obtained by doing simulations and experimental tests. The total thickness of the molding is 5.5mm. Fig. 5 shows the cross sectional structure of the Motion-SPM™ module in SIP packaging.

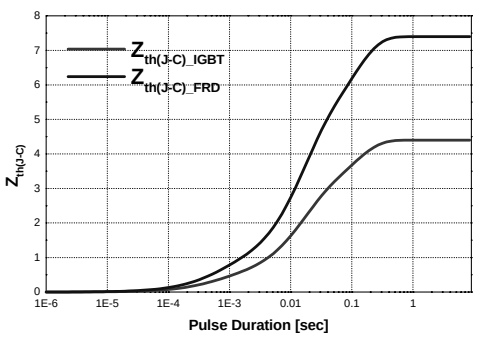

Fig. 4. Thermal impedance characteristic: junction to case of a 600V/8A rating device.

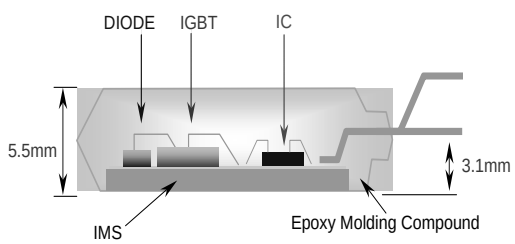

Fig. 5. Cross sectional structure.

The Motion-SPM™ module in SIP packaging provides two types of lead forms. One is Y-forms lead and the other type is L-forms lead. It takes advantage of the free arrangement of heat-sink as well as PCB design flexibility. Fig. 6 shows the lead forms of the Motion-SPM™ in SIP.

2.4 Isolating Consideration

For the design of the Motion-SPM™ module in SIP, isolation distances of pin-to-pin and pin-to-heatsink should be considered. As shown in Fig. 7(a), clearance and creepage distances of pin-to-heatsink are 3.10mm and 4.08mm respectively. As shown in Fig. 7(b), clearance and creepage distances of pin-to-pin are 2.35mm and 4.15mm respectively.

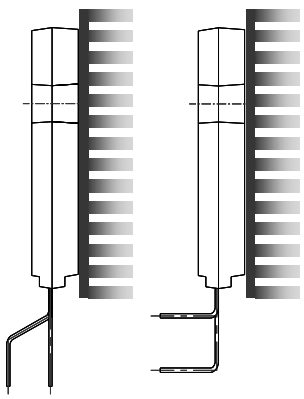

(a) (b)

Fig. 6. Lead forms of Motion-SPM™ in SIP.
(a) Y-forms (b) L-forms

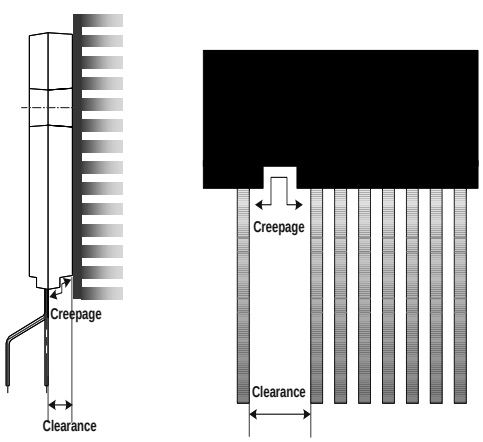

(a) (b)

Fig. 7. Isolation distance: (a) Pin-to-Heatsink (b) Pin-to-pin.

3. Electrical Performance and Power Ratings

3.1 Electrical Characteristics

The NPT IGBTs and ultra fast recovery diodes are designed for fast switching without excessive ringing. The turn-on and turn-off switching waveforms at the conditions of V_{DC}=300V, I_C=8A, V_{CC}=15V and T_j=150℃ is shown in Fig. 8. The Motion-SPM™ module in SIP packaging does not have current oscillation due to a moderate dv/dt rate to reduce EMI problems.

Fig. 9 shows the graph indicating the variation of switching dv/dt rates with switching current at the conditions of V_{DC}=300V and V_{CC}=15V. The turn-on and turn off dv/dt have values in the range of 2~4.5kV/us and 1~6kV/us.

Fig. 10 shows a switching loss at the condition of V_{CC}=15V and V_{DC}=300V. Based on the real experimental data, the single IGBT power loss and allowable output current according to the switching frequency was calculated. The procedure used for this calculation is briefly described below.

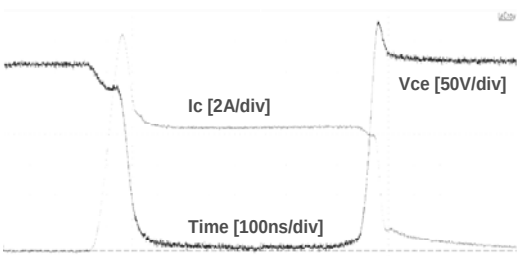

Fig. 8. Switching Waveform of 600V/8A rating device at V_{DC}=300V, I_C=8A, V_{CC}=15V, and T_j=150℃.

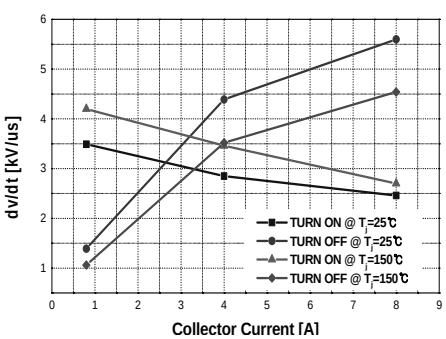

Fig. 9. Switching dV/dt rates of 600V/8A rating device at V_{DC}=300V, and V_{CC}=15V.

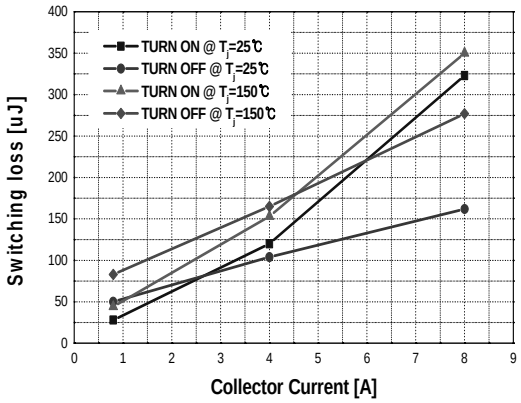

Fig. 10. Switching loss of 600V/8A rating device at V_{DC}=300V, and V_{CC}=15V.

3.2 Power Rating

The power-carrying potential of a device is dependent on the heat transfer capability of the device. The proposed module provides not only good thermal performance but also operating frequency options in accordance with the application.

The single IGBT power loss is composed of conduction and switching losses caused in the IGBTs and FRDs. The loss during the turn-off steady-state can be ignored because it is a very small amount and has little effect on increasing the temperature in the device. The conduction loss depends on the DC electrical characteristics of the device i.e., the saturation voltage. Therefore, it is a function of the conduction current and the device's junction temperature. Conversely, the switching loss is determined by the dynamic characteristics, such as turn-on/off time and over-voltage/current. Hence, in order to obtain the accurate switching loss, we should consider the DC-link voltage, the applied switching frequency, and the power circuit layout in addition to the current and temperature. Based on a PWM-Inverter system for motor control applications, the detailed equations are shown to calculate both losses of Motion-SPM^{TM} in SIP. The 3-phase continuous sinusoidal PWM is adopted [5]-[7].

3.2.1 Conduction Loss

The typical characteristics of forward drop voltage are approximated by the following linear equation for the IGBT and the diode, respectively.

$$\begin{aligned} v_I &= V_I + R_I \cdot i \\ v_D &= V_D + R_D \cdot i \end{aligned} \tag{3.1}$$

where V_I = Threshold voltage of IGBT, V_D = Threshold voltage of diode, R_I = on-state slope resistance of IGBT, and R_D = on-state slope resistance of diode.

Assuming that the switching frequency is high, the output current of the PWM-inverter can be assumed to be sinusoidal. That is,

$$i = I_{pk}\cos(\theta - \phi) \tag{3.2}$$

where is the phase-angle difference between output voltage and current. Using equations (3.1), the conduction loss of one IGBT and diode can be obtained as follows.

$$P_{con.I} = \frac{V_I I_{pk}}{2\pi}\int_{-\frac{\pi}{2}+\phi}^{\frac{\pi}{2}+\phi}\xi\cos(\theta-\phi)d\theta + \frac{R_I {I_{pk}}^2}{2\pi}\int_{-\frac{\pi}{2}+\phi}^{\frac{\pi}{2}+\phi}\xi\cos^2(\theta-\phi)d\theta \tag{3.3}$$

$$P_{con.D} = \frac{V_D I_{pk}}{2\pi}\int_{-\frac{\pi}{2}+\phi}^{\frac{\pi}{2}+\phi}(1-\xi)\cos(\theta-\phi)d\theta + \frac{R_D {I_{pk}}^2}{2\pi}\int_{-\frac{\pi}{2}+\phi}^{\frac{\pi}{2}+\phi}(1-\xi)\cos^2(\theta-\phi)d\theta \tag{3.4}$$

where ξ is the duty cycle in the given PWM method.

$$\xi = \frac{1+MI\cos\theta}{2} \tag{3.5}$$

where *MI* is the PWM modulation index (*MI*, defined as the peak phase voltage divided by half of the DC link voltage). Finally, the integration of equation (3.3) and (3.4) gives

$$\begin{aligned} P_{con} &= P_{con.I} + P_{con.D} \\ &= \frac{I_{pk}}{2\pi}(V_I + V_D) + \frac{I_{pk}}{8}(V_I - V_D)MI\cos\phi \\ &\quad + \frac{{I_{pk}}^2}{8}(R_I + R_D) + \frac{{I_{pk}}^2}{3\pi}(R_I - R_D)MI\cos\phi \end{aligned} \tag{3.6}$$

It should be noted that the total inverter conduction losses are six times that of the P_{con}.

3.2.2 Switching Loss

Different devices have different switching characteristics and they also vary according to the handled

voltage/current and the operating temperature/frequency. However, the turn-on/off loss energy (Joule) can be experimentally measured indirectly by multiplying the current and voltage and integrating over time, under a given circumstance. Therefore the linear dependency of a switching energy loss on the switched-current is expressed during one switching period as follows.

$$Swtitching \quad energy \quad loss = (E_I + E_D) \times i \quad [joule] \tag{3.7}$$

$$E_I = E_{I.ON} + E_{I.OFF} \tag{3.8}$$

$$E_D = E_{D.ON} + E_{D.OFF} \tag{3.9}$$

where $E_I i$ is the switching loss energy of the IGBT and E_D i is for the diode. E_I and E_D can approximately be considered a constant.

As mentioned in the above equation (3.2), the output current can be considered as a sinusoidal waveform and the switching loss occurs every PWM period in the continuous PWM schemes. Therefore, depending on the switching frequency of f_{SW}, the switching loss of one device is shown in the following equation (3.10).

$$P_{sw} = \frac{1}{2\pi} \int_{-\frac{\pi}{2}+\phi}^{\frac{\pi}{2}+\phi} (E_I + E_D)\ i\ f_{sw} d\phi \tag{3.10}$$

$$= \frac{(E_I + E_D) f_{sw} I_{pk}}{2\pi} \int_{-\frac{\pi}{2}+\phi}^{\frac{\pi}{2}+\phi} \cos(\theta - \phi) d\phi = \frac{(E_I + E_D) f_{sw} I_{pk}}{\pi}$$

where E_I is a unique constant of IGBT related to the switching energy and the different IGBT has different E_I value. E_D is one for each diode. Those should be derived by experimental measurement. From equation (3.10), it should be noted that the switching losses are a linear function of the current and directly proportional to the switching frequency.

3.2.3 Simulation and Experimental Results

It should be noted that the PWM modulation index MI = 0.8, cosϕ=0.8, V_{DC}=300V, V_{CC}=15V, I_{PK}=8A, T_j=150℃, f_{sw}=20kHz, sinusoidal output current are used as common simulated parameters in all the calculations. For the experimental setup, a TMS320C33 DSP controller, 5HP squirrel-cage induction motor, and 10kW dynamo are used. The induction motor controller is based on a conventional field-oriented method [8]-[9]. The device's junction temperature is below 150℃. Fig. 11 (a) shows the single IGBT power loss characteristics of a 600V/8A rating devices. Fig. 11 (b) shows the maximum peak current versus case temperature of the device by simulation results. These values are obtained based on typical experimental data. Fig. 11 (b) indicates the allowable peak current according to the case temperature of the device below the maximum junction temperature of the device under a given test condition. If the case temperature of the device is about 118℃, the allowable maximum peak current is 8A below T_j=150℃ condition. Fig. 12 (a) and (b) show the experimental results of the actual U-phase current and case temperature respectively. It is clear that the experimental results are much similar to the simulation results.

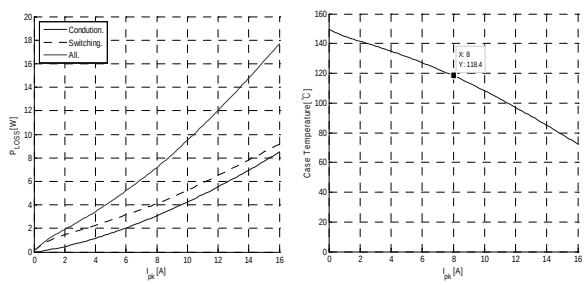

(a) (b)

Fig. 11. Simulation results of 600V/8A rating devices at V_{DC}=300V, V_{CC}=15V, f_{sw}=20kHz, and T_j=150℃: (a) Power loss (b) Allowable peak current

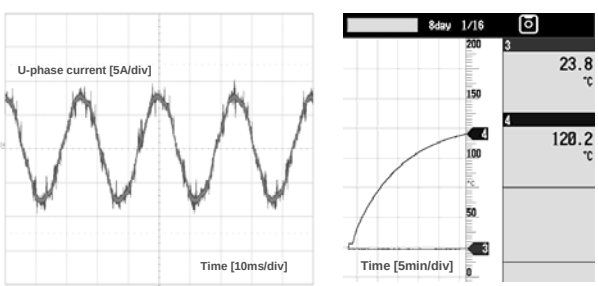

(a) (b)

Fig. 12. Experimental results of 600V/8A rating devices at V_{DC}=300V, V_{CC}=15V, f_{sw}=20kHz, and T_j=150℃: (a) U-phase current (b) Case temperature

3.3 Short-Circuit Ruggedness and Protection

The proposed module has one or three divided negative DC terminals to monitor the inverter leg current by using an external shunt resistor. The LVIC monitors the low-side collector current with the C_{SC} pin.

Fig. 13 (a) shows the actual waveforms under a short-circuit protecting situation with an external shunt resistor, R_{SC}=20mΩ. Once the voltage across R_{SC} reaches 0.5V, the LVIC shuts down the gating signal after a time delay of about 1.3us. This is composed of the LVIC internal filter and the externally added low-pass filter. If there is not a protection circuit, as shown in Fig. 13 (b), it is noted that the IGBT within the Motion-SPM^{TM} module in SIP package is destroyed after a short-circuit withstanding time of about 5us.

4. Overall Application Circuit

4.1 Overall Application Circuit

The circuit configuration for a typical application is shown in Fig. 14. A single-supply 15V drives the low-side IGBTs directly and charges the bootstrap circuitry for the HVICs. The HVIC and LVIC block the command signals from the controller and generate a fault signal when the type of failure mode, i.e. the SC current failure or the supply under-voltage failure, is detected. To prevent surge destruction, the wiring between the smoothing capacitor and the P/GND pins should be as short as possible. The use of a high frequency non-inductive capacitor of around 0.1~0.22uF between the P/GND pins is recommended.

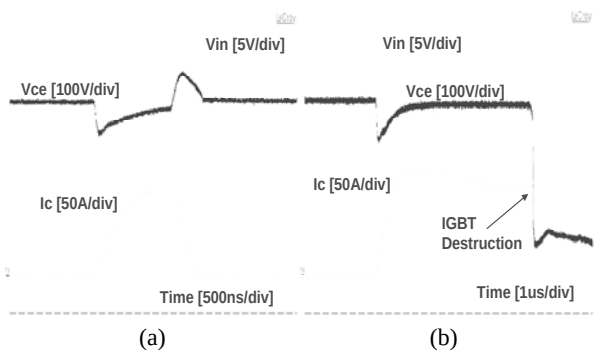

Fig. 13. Short Circuit Test results of 600V/8A rating devices at V_{DC}=450V, V_{CC}=20V, and T_j=150℃:
(a) Protected waveform (b) Destructed waveform

4.2 Recommended Input Connection Design

The integrated 5V CMOS/TTL compatible Schmitt trigger input conditioning circuit enables easy interface with a microprocessor. The input signal is a High-Active Type. There is a 5kΩ resistor inside the IC to pull each input signal line down to GND. RC coupling circuits should be adopted for the prevention of input signal oscillation. The time constant of RC coupling circuits should be selected in the range of 50~150ns. The recommended values of RC coupling circuits are 100Ω for the resistor and 1nF for the capacitor. The VFO output is an open collector type. This signal line should be pulled up to the positive side of the 5V power supply with an approximately 2kΩ resistor and pulled down to GND with a 4.7nF capacitor for fault and temperature detection. Fig. 15 shows the example of a connection to a microprocessor.

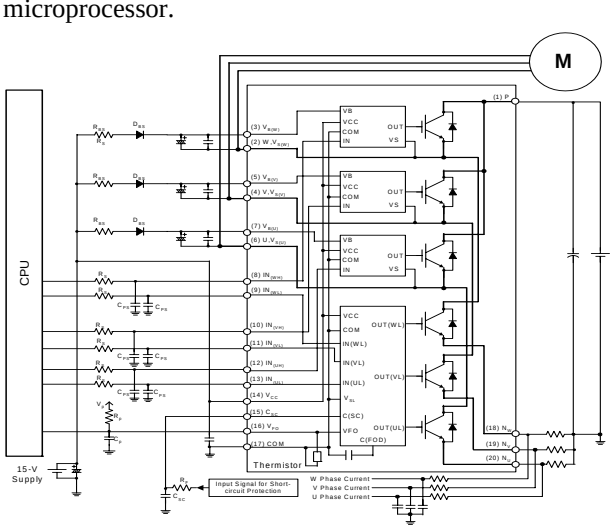

Fig. 14. A Typical Application circuit for 3-N type of Motion-SPM^{TM} in SIP.

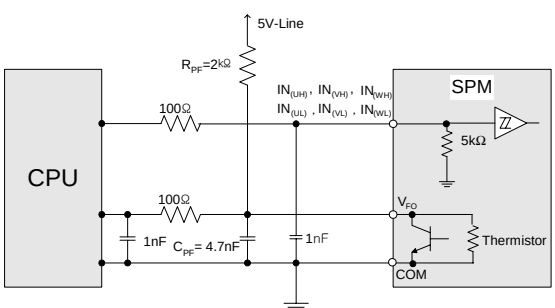

Fig. 15. Example of connection to a microprocessor.

5. Conclusions

In this paper, an overall description to the Motion-SPM™ module in SIP packaging is presented. This module offers tremendous advantages such as increased reliability, design flexibility, simple construction, easy assembly, and cost-effectiveness of the inverter power stage for home appliance applications. It uses six NPT 600V IGBTs, six freewheeling diodes, three HVICs, one LVIC and one thermistor. For the user's design pliability, the Motion-SPM™ module in SIP packaging offers two types of negative DC terminals and lead forms. The electrical characteristics such as switching performance, single IGBT power loss, power rating and short circuit ruggedness is investigated. The Motion-SPM™ module in SIP packaging provides an excellent solution for appliance motor drives and other light industrial drive applications.

References

[1] Tae-Sung Kwon, Jun-Ho Song, Jun-Bae Lee, Seung-Han Paek and Sung-Il Yong, "A New Smart Power Module for Low Power Motor Drives," ICPE'07, pp. 695-699, 22-26 Oct. 2007.

[2] JB.Lee, BC.Cho, DW.Chung, BS.Suh, "Improved Smart Power Modules for up to 7kW Motor Drive Applications," PESC, 2006.

[3] J.B.Lee, B.C. Cho, D.W. Chung and B.S.Suh, "Design of a High-side Gate Driver using a Mini-SPM," IPEC 2005, pp. 1619-1623, 2005.

[4] Jong-Tae Hwang, "High Noise Immunity High-Side Gate Driver IC," *Power Systems Design Europe*, pp.24-28, May 2005.

[5] F. Casanellas, "Losses in PWM inverters using IGBT's," *Proc. Inst. Elect. Eng.-Elect. Power Applicant.*, Vol.141, No. 5, pp. 235-239, Sep. 1994.

[6] K. Berringer, J. Marvin and P. Perruchoud, "Semiconductor Power Losses in AC inverters," *Conf. Rec. of IEEE IAS'95*, pp. 882-888, 1995.

[7] Smart Power Module motion SPM user's guide, application note AN9035, Fairchild Semiconductor

[8] Jong-Gyu Park, Jae-Ho Chung, Hwi-Beom Shin, "Anti-windup Integral-Proportional Controller for Variable-Speed Motor Drives," *Journal of Power Electronics*, Vol. 2, No. 2, pp.130-138, 2002.

[9] Sang-Uk Kim, Jin-Ho Choi, Young-Seok Kim, "Vector Control of Induction Motors using Optimal Efficiency Control," *Journal of Power Electronics*, Vol.2, No.1, pp.67-75, 2002.

Tae-Sung Kwon received his B.S. degree in Electrical Engineering from Incheon University, Incheon, Korea, in 2002, and his M.S. degree in Electrical Engineering from Hanyang University, Seoul, Korea, in 2004.

From 2004 to 2005, he was with the Korea Automotive Technology Institute, Cheonan, Korea, as a Research Engineer in the Electronic System R & D Center, R & D Division. He is currently with Fairchild Korea Semiconductor, Bucheon, Korea, where he is a Senior Research Engineer in the Motion Control System Team, HV PCIA. His primary areas of research include power devices in high voltage, drive ICs, power modules, and motor drives.

Sung-Il Yong received his B.S. and M.S. degrees in Electrical Engineering from Seoul National University, Seoul, Korea, in 1992, 1994, respectively. During 1994-2000, he was a senior engineer with Samsung Electronics in Suwon, Korea. During 2001-2002, he was a principal engineer with Huropec (a spin off company from Samsung Electronics) in Suwon, Korea. Since 2003, he has been working for Fairchild Semiconductor as a director of the SPM business unit.